Atomic force microscopy study of 60-keV Ar-ion-induced ripple patterns on Si(100)

Debi Prasad Datta and Tapas Kumar Chini*
Surface Physics Division, Saha Institute of Nuclear Physics, 1/AF Bidhannagar, Kolkata 700 064, India
(Received 9 October 2003; revised manuscript received 17 February 2004; published 16 June 2004)

The evolution of a ripple pattern on Si(100) surfaces induced by 60 keV Ar^+ beam incident at 60° with the surface normal has been studied as a function of bombardment time using *ex situ* atomic force microscopy (AFM) in ambient condition. The ripple wavelength (l) and roughness amplitude (W) increase with bombardment time following a scaling law $l \propto t^{\gamma}$ and $W \propto t^{\beta}$, where $\gamma = 0.64 \pm 0.08$ to a crossover value 0.22 ± 0.07 and $\beta = 0.76 \pm 0.03$ to a crossover at 0.27 ± 0.11. The ripple orientation and average wavelength observed in the early stage patterned morphology can be described by a linear continuum model. However, the scaling exponents for the power law variation of roughness amplitude and wavelength with bombardment time are not consistent with predictions of the linear model or the Kuramoto-Sivashinsky-equation-based nonlinear model.

DOI: 10.1103/PhysRevB.69.235313 PACS number(s): 79.20.Rf, 61.82.Fk, 81.16.Rf, 68.35.Ct

I. INTRODUCTION

In the process of obliquely incident ion bombardment (eV to keV region) of a solid surface, the development of spontaneous ripple or wavelike morphology with spatial periodicity ranging from nm to μm scale has become a topic of intense research in recent years, due to the fact that such a self-organized surface pattern may open a simple and inexpensive route to fabricate useful nanoscale textured materials, such as templates for one-dimensional structures.[1] Ion-induced ripples are thought to be produced as a result of the interplay between a roughening process[2] caused by surface-curvature-dependent ion erosion (called sputtering) of the surface and a smoothing process[2,3] via surface diffusion.

Much attention[3–5] has been paid to the understanding of the dynamics of a ripple pattern on surfaces developed by ion erosion using the theories developed for nonequilibrium surfaces/interfaces generated in growth[6] processes. Based on the continuum theory of ion-beam sputtering by Sigmund,[7] recently, Cuerno and Barabasi (CB)[3] or more generally Makeev, Cuerno, and Barabasi (MCB)[4] have developed a model to describe the ion-induced pattern formation on amorphous or semiconductor materials which are amorphized easily by ion bombardment. If crystallinity induced anisotropic diffusion is included,[5] the CB model can also be applied to describe ion-induced patterning on metal surfaces. The early stage morphology predicted in the CB model[3] is identical with the linear instability theory, originally developed by Bradley and Harper (BH),[2] that predicts the formation of ripple pattern oriented perpendicualar or parallel to the projection of ion beam onto the surface of amorphous material for obliquely incident ion beam. However, the late stage dynamics of the ion-induced morphology is dominated by the nonlinear terms of the Kuramoto-Sivashinsky (KS) equation[8] involved in the CB model[3] as described by Park *et al.*[9] and Rost and Krug.[10] Depending on the sign of the product of the coefficients of the two nonlinear terms, the late stage morphology may show[3,9,10] kinetic roughening to be described by the universality class of the Kardar-Parisi-Zhang (KPZ) equation[11] or yield the formation of rotated ripple structure (RRS) (Refs. 9 and 12) or dots and hole[13] on the ion eroded surface. However, a recent atomistic Monte Carlo (MC) simulation study on the ion-induced surface morphology in $2+1$ dimensions by Hartmann *et al.*[14] has shown that it is the nature of the surface diffusion which decides whether the ripple pattern formed in early time will survive or undergo a non periodic rough morphology for long time bombardment.

While the predictions of the linear theory are to some extent in agreement with the recent experiment, [15,16] satisfactory experimental results conforming the predictions of nonlinear theory are scarce[16] and in some cases conflicting.[17] Thus, the late stage dynamics of ion-beam-induced patterned morphology remains a debatable issue and needs more experimental data for testing the theoretical models and controlling the pattern formation on solid surface via ion beam route. The purpose of the present paper is to focus on the experimental investigation of the morphology development for medium keV Ar bombardment on Si at oblique angle of ion incidence for sufficient long time to explore various features to be expected in late stage morphology of the ion-sputtered surface.

II. EXPERIMENTAL

The ion bombardment of Si targets [p-type Si(001) single-crystal wafer] was undertaken with a high current ion implanter (Danfysik) which is described in detail elsewhere.[18] The Si samples were irradiated with 60 keV $^{40}Ar^+$ ions at 60° angle of ion incidence with respect to surface normal of the samples. The ion flux was kept constant at around 175 μA cm^{-2} for all irradiations and ion fluence up to $\sim 3.0 \times 10^{19}$ ions cm^{-2} was chosen that covers a sufficient long bombardment time (more than 8 h). Homogeneous irradiation was achieved via two-dimensional magnetic sweeping system. The Si samples were clamped onto a copper block heat sink but such mounting arrangement does not ensure good thermal contact. As a result, temperature of the sample may rise around 150 °C due to beam heating for prolong bombardment. After irradiation, the surface topography of the samples were investigated by atomic force microscopy (AFM) in contact mode under ambient condition as described earlier.[18,19]

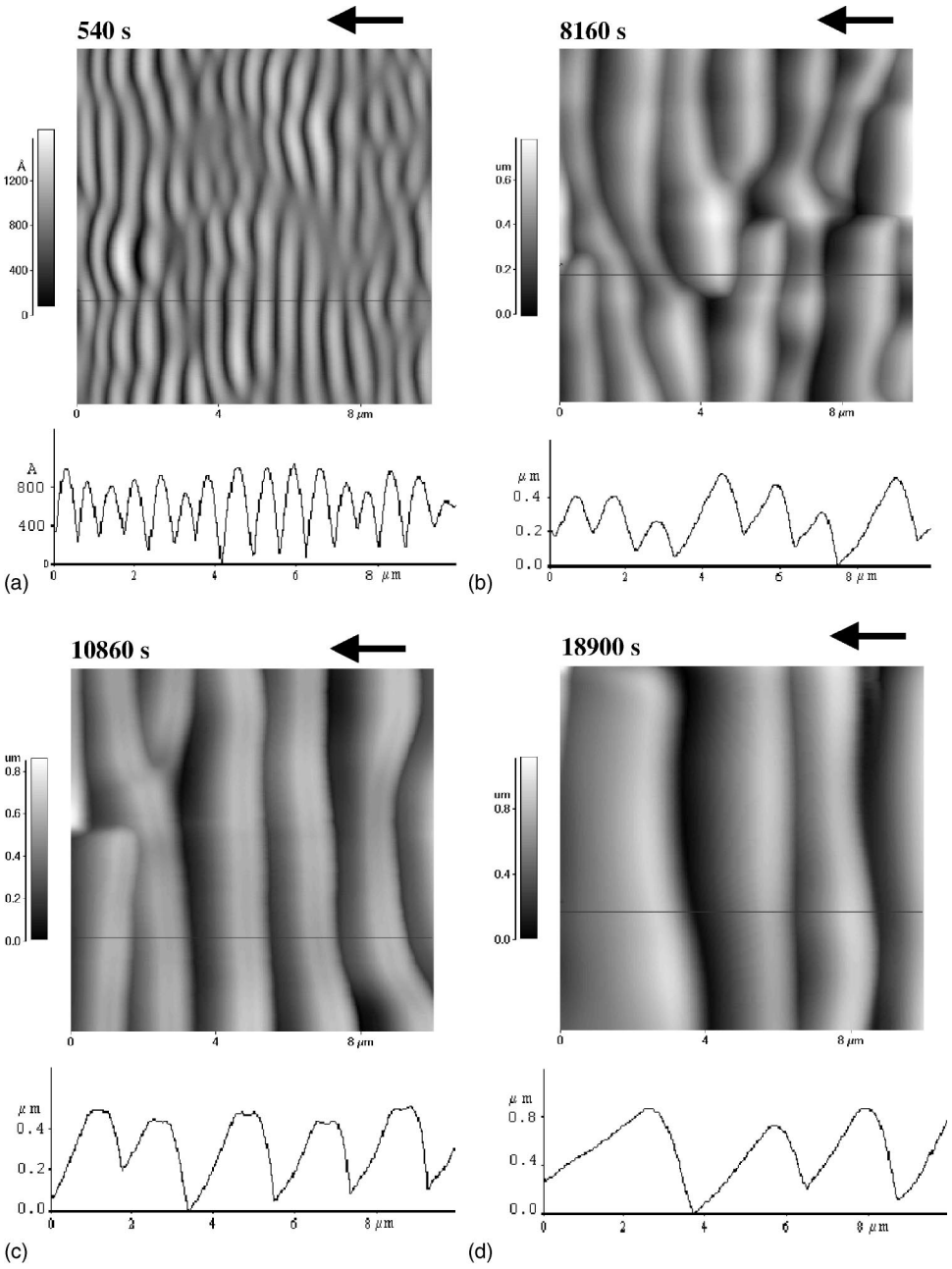

FIG. 1. AFM images of the Si surfaces for different bombardment times with a fixed ion flux of 175 μA cm^{-2}.

III. RESULTS

Before irradiation the surfaces of the Si samples exhibited a root-mean-square (rms) roughness of $\sim$0.2 nm. A correlated periodic morphology starts to appear after a sputtering time, $t \sim 440$ s corresponding to a fluence $\sim 4.0 \times 10^{17}$ ions cm^{-2} for the ion flux of 175 μA cm^{-2} used in the present experiment. In Figs. 1(a)–1(d) we report four AFM images taken at different times to follow the surface evolution versus the sputtering time. A representative quasiperiodic ripple pattern from an early time morphology is presented in Fig. 1(a) for sputtering time of 540 s. As the sputtering proceeds the spatial periodicity or the wavelength increases and the regular ripple pattern starts to be distorted as shown in the AFM image of Fig. 1(b) after a sputtering time of 8160 s. However, if the sputtering is continued, the morphology looks more similar to a faceted ripple pattern as displayed in Figs. 1(c) and 1(d) that remains stable for long-time sputtering upto 30 300 s. Close inspection of the line scans or the height profiles shown under each AFM image of Fig. 1 as a function of sputtering time reveals that habit of surface pattern is changed from sinusoidal [Fig. 1(a)] to triangular [Fig. 1(b)] and sawtoothlike [Fig. 1(d)]. Moreover, in all the stages of the evolution of ripple pattern the orientation of the ripples are always perpendicular to the projection of ion beam flux on to the surface as indicated by the arrow marks on each AFM images of Figs. 1(a)–1(d).

To quantify the observed ripple pattern we study the scaling properties of the interface as done in Refs. 20–22 for surfaces with a periodic (mound) morphology. We evaluate the height difference correlation function[21] $G(r)$ of the AFM data, with $G(r) = \langle (h_i - h_j)^2 \rangle$, where h_i and h_j are the heights

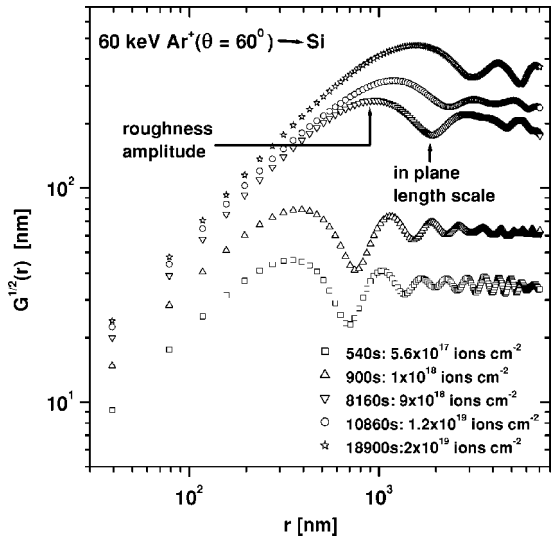

FIG. 2. Square root of the height difference correlation function $G(r)$ of the surfaces bombarded for different times. Each correlation function is the average over many AFM images taken from different areas of a surface. Arrows mark (i) the distance $r=d$ that gives the first local minimum of $G^{1/2}(r)$ and (ii) the surface roughness amplitude $W=G^{1/2}(d/2)$.

of the surface at two locations separated by a distance r, and the brackets signify an average over pairs of points i and j. The dynamic scaling hypothesis states[21] that for r smaller than the length scale of average separation of the periodic features $G(r)\propto r^{2\alpha}$, where α is called the roughness exponent. Examples of $G^{1/2}(r)$ calculated from the AFM images of the surfaces sputtered for different times are plotted in Fig. 2. In order to avoid sampling-induced oscillations[23] in the $G(r)$, care has been taken to include many AFM images in the averaging of $G(r)$ data. In our analysis we have checked that 4 to 6 AFM images from each sample are enough to give statistically reliable data to obtain $G(r)$ plot. The correlation function here is calculated along the projection of the ion beam direction (the other direction is averaged out) on to the surface as indicated by the arrow marks in Fig. 1. The roughness exponent α was determined from a fit to the linear part of the log-log plot of $G^{1/2}(r)$ vs r. The α remains nearly time invariant yielding an average value of 0.92. Following the method described in Ref. 22, we define the surface roughness amplitude W (shown with upward arrow mark in Fig. 2) as the value of $G^{1/2}(r)$ at the first local maximum, $W=G^{1/2}(d/2)$, where the characteristic in-plane length scale d (upward arrow mark in Fig. 2) is the position of r at the first local minimum of $G^{1/2}(r)$. This definition of roughnes amplitude is preferred over the large r limit of $G^{1/2}(r)$ because AFM data can be affected by artifacts at large length scales. The average peak-peak separation of the oscillations observed in the $G^{1/2}(r)$ vs r plot (Fig. 2) is considered as the measure of ripple wavelength l in the present study. At later times of the sputtering shown in Fig. 2, there exists a first minimum but not a clear periodic oscillation, and therefore the measurement of l in the late stage pattern development can become somewhat irrelevant. In the late stage pattern development we thus adopt d, the in-plane

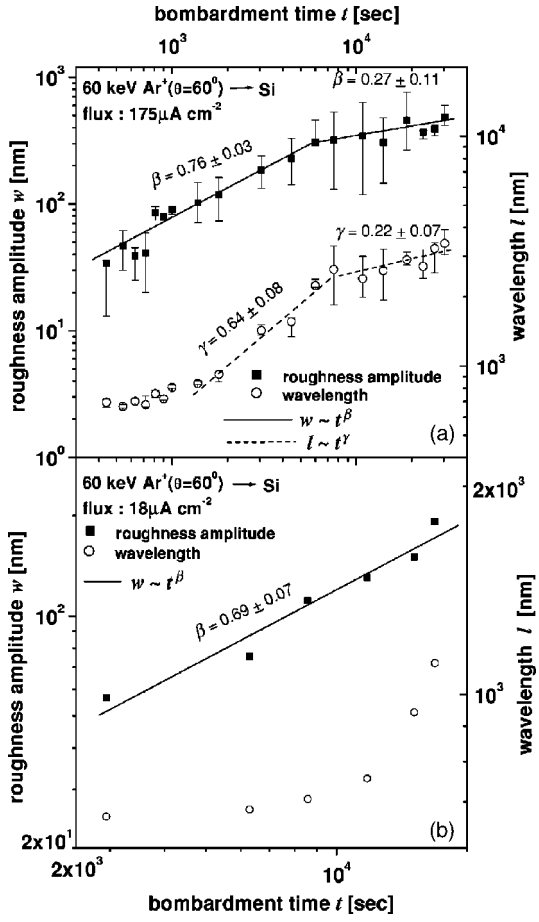

FIG. 3. The ripple wavelength l and the surface roughness amplitude W as a function of bombardment time. Ion flux (a) =175 μA cm^{-2} and (b) =18 μA cm^{-2}.

length scale as a rough measure of wavelength l of the irregular periodic pattern.

In Fig. 3(a), we report the variation of roughness amplitude W as a function of sputter time t showing a power law behavior $W\propto t^{\beta}$ together with the time scaling behavior of the ripple wavelength $l\propto t^{\gamma}$ for the ion flux of 175 μA cm^{-2}. According to the scaling theory,[6] β is called the growth exponent and reciprocal of γ is the dynamic exponent. Clearly, we can recognize a crossover in the power law scaling of W from $\beta=0.76\pm0.03$ to $\beta=0.27\pm0.11$. Further, the wavelength of the ripple pattern underlies a coarsening process with $\gamma=0.64\pm0.08$ to a crossover value of 0.22 ± 0.07. Figure 3 shows that the wavelength of the ripple pattern in the present study varies from about 700 to 3500 nm while the roughness amplitude varies from about 30 to 500 nm. Also, with respect to ripple pattern evolution we can classify three time regimes from the Fig. 3(a). (1) Early time regime where the average wavelength of ripple pattern remains more or less constant in the sputtering time region ~440–750 s (fluence range $\sim4.0\times10^{17}-8.0\times10^{17}$ ions cm^{-2}), (2) intermediate time regime extends from ~800 s up to ~6000 s. The growth exponent $\beta=0.76$ covers both the early and intermediate time regime, wheras the exponent $\gamma=0.64$ covers intermediate time regime. (3) The late time regime morphology spans from ~6000 s to ~30 300 s. The crossover values of β and γ fall in this regime.

IV. DISCUSSION

The height evolution $h(x,y,t)$ of a sputter eroded amorphous material or semiconductor surface (amorphizable by ion bombardment) is well approximated[3,4] by the noisy version of the anisotropic KS equation,[8]

$$\partial_t h = \nu\nabla^2 h - (D^T + D^I)\nabla^4 h + \frac{\lambda}{2}(\nabla h)^2 + \eta(x,y,t). \quad (1)$$

Here ν is the roughening prefactor (also called effective surface tension), generated by the ion bombardment sputter-erosion process. D^T and D^I are designated as thermally activated surface diffusion constant and ion induced effective surface diffusion (ESD) constant. The nonlinear term λ represents the slope dependent erosion rate, where (∇h) define the local slopes and $\eta(x,y,t)$ is an uncorrelated white noise with zero average, mimicking the local random fluctuation of the incident ion flux. All the coefficients of Eq. (1) can be made directional in (x,y) space and their detailed expressions are known.[4] Numerical simulation of the Eq. (1) reveals a clear separation in time of the linear and nonlinear behaviors. Before a characteristic time $t<t_c$,[9] nonlinear and noise terms can be neglected ($\lambda=0, \eta=0$) and Eq. (1) reduces to the linear BH theory[2] except for the fact that surface diffusion constant K has two components $K=D^I+D^T$. In the linear regime the balance of the unstable negative sputter-erosion term $(-|\nu|\partial^2 h)$, trying to roughen the surface and the positive surface diffusion term $(K\nabla^4 h)$ acting to smooth the surface, gives rise to observable ripple with wavelength $l_i = 2\pi\sqrt{2K/|\nu_i|}$, where i refers to the direction (x, the projected direction of the ion beam, or y) along which the associated $|\nu_i|$ ($|\nu_x|$ or $|\nu_y|$) is largest. However, beyond the crossover time, i.e., $t>t_c\sim(D/\nu^2)\ln(\nu/\lambda)$, the results of Park *et al.*[9] shows that the nonlinear terms completely determines the surface morphology.

Using the present experimental parameters, such as beam energy $\epsilon=60$ keV, flux $f=175$ μm cm^{-2}, ion incident angle $\theta=60°$, and average penetration depth along the beam direction $a=82$ nm calculated from TRIM 2003[24] and the material specific constant $p=1.7\times10^{-3}$ nm^4 eV (Ref. 4) for Si, we estimate the magnitude of different coefficients[4] $D_x^I=2.6\times10^4$ nm^4 s^{-1}, $D_y^I=6.9\times10^2$ nm^4 s^{-1}, $\nu_x=-18$ nm^2 s^{-1}, $\nu_y=-6.57$ nm^2 s^{-1}, and $\lambda_x<0, \lambda_y<0$. Here, we have assumed the width of the energy distributions along and perpendicular to beam direction as $\sigma=a/2$ and $\mu=a/4$ which means an asymmetric distribution closer to the more realistic situation.[2] The calculated D_x^I in the present case is three order of magnitude higher than the estimated[15] thermally activated surface diffusion constant, $D^T=34$ nm^4 sec^{-1} at 550 °C for Si(100). Thus ion induced ESD is dominant over the thermally activated surface diffusion in the present experiment. We observed the ripple wavelength in the early time to be independent of the ion flux [Fig. 3(b)] which is also a signature of the dominance of the ion induced ESD process over the thermal diffusion. As $|\nu_x|>|\nu_y|$, we should have $l_x = 2\pi\sqrt{2D_x^I/|\nu_x|}=2\pi\sqrt{2}l_c$, where $l_c(=\sqrt{D_x^I/|\nu_x|})$ is called the characteristic length scale[3] in the system. The calculated l_x is $\sim$337 nm, a factor of $\sim$2 smaller than the observed ripple wavelength ($\sim$700 nm), a reasonably good agreement between theory and experiment. The orientation of the observed ripple pattern (Fig. 1) and that its wavelength remains almost constant in the sputtering time range 400–800 s (corresponding dose range 4.0×10^{17}-8.0×10^{17} ions cm^{-2}) as depicted in Fig. 3(a) is consistent with the early time ripple dynamics predicted by the linear version of the CB (Ref. 3) or BH (Ref. 2) theory. However, BH predicted exponential increase of roughness amplitude in the early time is not observed in our case, instead, a power law increase of the amplitude prevails in early as well as intermediate time with the same value of the exponent β. The power law exponent $\beta=0.76$ observed here in early as well as intermediate time regime differs from the early time $\beta=0.25$ obtained by Chan and Wang[25] for roughness evolution on 500 eV Ar^+ bombarded Si(111) surface where no ripple topography is developed. But it should be noted that normal incidence ion beam was employed in the experiment of Ref. 25 where the surface roughening is isotropic in great contrast to the anisotropic morphology observed in our case of ion bombardment at 60° (with respect to the surface normal of the sample). Also the etch rate is much less than one bilayer per minute in the work of Ref. 25. Regarding the very early stage pattern development and the corresponding variation of the roughness amplitude and wavelength with time to be expected in our experiments remain an open question because the smallest reproducible adjustable sputter time for 175 μA cm^{-2} flux used was $\sim$440 s.

For a high oblique ion incident angle, such as 60° as used in the present case, an important issue which should be considered for ripple evolution beyond linear regime is the effect of shadowing.[17] As the amplitude to the wavelength ratio (W/l) increases with time, the maximum gradient of the sinusoidal surface profile gradually becomes too large causing a part of the upstream face of the sinusoidal ripple being shadowed from incident ion flux by the preceding peak in the wave. For a sinusoidal ripple approximated by $h=W\sin(2\pi x/l)$ Carter[26] has shown that the limiting condition for such shadowing not to occur is $\tan(\pi/2-\theta)\geqslant 2\pi W/l$ which places an upper limit on W/l for any ion incidence angle θ (with respect to the surface normal of the initial macroscopic flat surface). Here, $\tan\alpha=\partial h/\partial x$ defines the local slopes and $2\pi W/l$ represents the maximum gradient or slope of the ripples. For the present experimental situation θ being 60°, the maximum tilt angle of the slope of the ripples should thus be $(\pi/2-\pi/3)=30°$ or $W/l\leqslant 0.09$ to avoid shadowing. Estimation of the W/l ratio from Fig. 2 shows that no shadowing occurs upto about 750 s. At 810 s the W/l ratio is about 0.1 implying that the average up or down slope of the ripples is $\tan\alpha=2\pi\times0.1\approx0.6$, corresponding to a tilt angle $\alpha=31°$. This clearly indicates that the shadowing process started around 800 s from where the wavelength starts to increase as observed in Fig. 3(a). In the present case, the sputtering time of 800 s, corresponding to the dose of $\sim8.5\times10^{17}$ ions cm^{-2}, can be taken roughly as a measure of the characteristic time t_c (Ref. 9) separating the linear and nonlinear regime. As $D\sim f$ (Ref. 4) and $\nu\sim f$,[4] f being the ion flux, we have $t_c\propto 1/f$. To test the tuning of t_c by varying f, the ion flux, we monitored [Fig. 3(b)] the variation of wavelength as well as the amplitude of the ripple formed at a flux reduced by 1/10th of the flux 175 μA cm^{-2}

used initially. From Figs. 3(a) and 3(b), by comparing the shift of the point at which the wavelength starts to increase one can realize that onset of the nonlinearity has almost increased by a factor of 10 accordingly. Presumably, the shadowing transition mentioned above as one goes from the early time to intermediate time region (Fig. 3), triggers a nonlinear process. Beyond 800 s, i.e., $t > t_c$, including intermediate and late stage, the average W/l ratio varies in the range 0.1–0.16 which is above the critical value (0.09) of shadowing under the present experimental condition. Thus, the transition from ripple to faceted patterned morphology observed here (Fig. 1) and the associated power law variation of the amplitude and wavelength of the correlated patterned features beyond 800 s of sputtering [Fig. 3(a)] can be thought solely due to shadowing. However, the faster growth rate of amplitude and wavelength at the intermediate time regime (800–6000 s) slows down to a moderate rate in the late time regime (6000–30 300 s). Other effects associated with shadowing may influence the late stages of dynamic evolution of the surface. These effects include redeposition of sputtered atomic flux from points of origin to other surface regions and scattered ion flux, which can enhance the incident external flux locally.[17] It has been pointed out by Carter[26] that if the W/l ratio exceeds the critical value of the shadowing condition, the valleys of the sinusoid will not be eroded but the peaks will be planarized resulting a flat top height profile, which is discernible from the late stage morphology shown in the AFM image of Fig. 1(c) and the height profile presented below it. Although the dynamics of the subsequent changes in the surface morphology are difficult to describe theoretically at this and subsequent stages it is reasonable to expect that a transformation to a sawtoothlike wave form will evolve.[26] Indeed, such a faceted morpholgy with sawtooth wave form is observed in the present work as depicted in the height profile of the AFM image of Fig. 1(d). Similar morphological transition under oblique ion bombardment has also been observed experimentally by other groups.[17,27,28]

For large time ($t > t_c$) and at large length scale ($l > l_c$) for $\lambda_x \lambda_y > 0$, as in the present case, a kinetic roughening with the power law increase of the roughness amplitude with time with unknown exponent[9] or the KPZ exponent with $\alpha \approx 0.38$ and $\beta \approx 0.25$ in 2+1 dimensions are predicted.[4] The presence of disordered or broken ripples as seen from the representative AFM image of Fig. 1(b) or a partial loss of long-range order in the later time of sputtering as observed in Fig. 2 may appear as a symptom of nonlinearity predicted in Ref. 9. However, we always see the presence of a local minima in the $G^{1/2}(r)$ vs r plot at different stages of the morphology development from the early to the late stage which implies that periodic surface pattern exists at all times. The first order nonlinear processes discussed by Cuerno *et al.*[3] or Park *et al.*[9] are vaild for slowly undulating surface (without ion flux shadowing) where the periodic ripple to nonperiodic roughening transition occurs in the late time morpholgy. However, in several surface areas where shadowing occurs as in the present case, neither the linear BH nor the first-order nonlinear KS equations [Eq. (1)] advocated by Cuerno *et al.*[3] are valid. In such situation it is expected[17] that higher-order nonlinear processes will be dominant beyond $t > t_c$ and as a result transition to a true kinetic roughening as

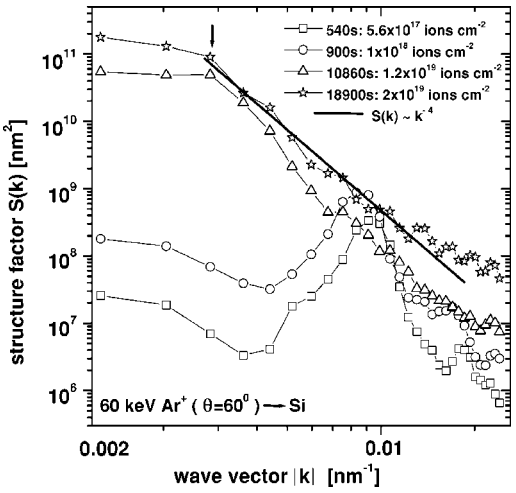

FIG. 4. Structure factor $S(k)$ calculated from AFM pictures with increasing bombardment time. $S(k)$ above the downward arrow mark follows k^{-4} law at late time regime of sputtering.

predicted in Refs. 3, 4, and 9 is never observed in the present study and also the wavelength coarsening with time as observed here is absent in the CB/MCB model.[3,4] So, a quantitative comparison with the observed scaling exponents (α, β) with the KPZ predicted exponents in large time scale is not warranted for the present results.

To gain further insight of the ripple morphology beyond the linear region and for detailed analyses of the AFM pictures (wavelengths, local slopes, etc.) the structure factor $S(k) = |\hat{h}(\mathbf{k})|^2$ of the height topography $h(\mathbf{r}, t)$ was computed, where $\hat{h}(\mathbf{k}) \propto \int_r \exp[i\mathbf{kr}][h(\mathbf{r}) - \overline{h}]d\mathbf{r}$. $S(k)$ was calculated for cuts through the AFM pictures along the ion-beam direction and is displayed in Fig. 4. The maximum of the structure factor $S(k)$ corresponds to the observed wavelength ($\sim$700 nm) in the linear regime similar to that observed in Refs. 12 and 16 for sputtering time 540 s (5.6×10^{17} ions cm^{-2}). For increasing fluence, the long-range corrugations with wavelengths $l_x > 2\pi\sqrt{2} l_c$ grow faster than the short-wave corrugations and shift the maximum of $S(k)$ to smaller wave vectors. To confirm the nonlinear surface evolution one should expect KPZ scaling behavior[3] $S(k) \propto |\mathbf{k}|^{-\nu}$ with $\nu = 2.7$ as is observerd experimentally in Ref. 16. However, the $S(k)$ behavior at the late stage morphology in our case does not conform this. Instead, $S(k)$ follows a power law dependece close to k^{-4}, above the wave vector (indicated by vertical downward arrow in Fig. 4) corresponding to the wavelength of the faceted or sawtooth ripple pattern observed at late time regime (after a sputtering time of 18 900 s). As no peak occurs in the $S(k)$ curve at late time regime, the usual concept of wavelength designated for a sinusoidal surface profile is not relevant here and the downward arrow mark shown in Fig. 4 represents the location of in plane length scale of patterned morpholgy observed beyond the linear regime.

Quite recently, the atomistic Monte Carlo (MC) simulation in (2+1) dimensions by Hartmann *et al.*[14] has shown that while the use of activated surface diffusion (ASD)[29] produces the transition from early time periodic ripple pattern to

late-stage rough morphology with KPZ scaling, the use of Wolf-Villain (WV)[30] type irreversible relaxation gives ripple morphology in early as well as late time similar to the present result. So, it is possible that different surface relaxation acting in different stages of morphology may be the important factor for the crossover of the β value from intermediate time to late time morphology in the present case. The ion induced ESD coefficient D^I being a function of ion flux and ion incidence angle should change with time as both the flux and and ion incidence angle change locally as the shadowing process dominates with time. However, the time dependence of D^I and how it affects the exponents β are not known. One of the most possible causes of the drastic change of surface relaxation may occur via enhancement of the surface adatom mobility by ion bombardment.[31] Coarsening of ripple wavelength having exponent, $\gamma=0.64$ in the intermediate time here is substantially higher than observed experimentally for 40 keV Xe^+ bombarded Si surface[17] and for low keV Ar^+ bombarded fused silica[32] or crystalline metal surfaces.[33] Ripple coarsening on crystalline metal surface, such as on Cu (Ref. 33) was attributed to anisotropic surface diffusion induced by a Ehrlich-Schwoebel (ES) barrier. However, in the present experimental condition an amorphous layer of more than 100 nm thickness extending from surface to the subsurface are produced[34] and ES barrier should not play a significant role for ripple wavelength coarsening on such amorphous material. Currently, we have no clear idea about the origin of the observed exponents for ripple coarsening.

V. CONCLUSIONS

In conclusion, the nature of ripple morphology induced by 60 keV Ar^+ beam at 60° angle of ion incidence on silicon surface has been studied by *ex situ* atomic force microscopy (AFM) under ambient condition as a function of bombardment time (fluence). A detailed analysis of the morphology of the ion eroded surface using an ion flux of 175 μA cm^{-2} shows the formation of regular ripple pattern in early time from 400 to 800 s (corresponding dose range $4.0\times10^{17}-8.0\times10^{17}$ ions cm^{-2}). For intermediate time bombardment up to 6000 s (6×10^{18} ions cm^{-2}) ripples are to some extent distorted and a partial loss of long range order in the periodic pattern is observed. Finally, for bombardment in late time regime, i.e., in 6000–30 300 s (up to 3.0×10^{19} ions cm^{-2}), morphology appears as a faceted wave pattern with a sawtoothlike surface profile. Beyond early time, the morphological transition has been attributed mainly to the shadowing effect. The variation of the roughness amplitude and wavelength of the periodic wave pattern with bombardment time follows a power law scaling and both the variations show a crossover at the late stage where scaling exponents are much smaller than that in the intermediate time. Beyond the early time (i.e., after about 800 s of sputtering with an ion flux of 175 μA cm^{-2}), the morphological evolution under the influence of shadowing processes cannot be explained with the existing models. The present experimental results, thus, demand for further investigation of the nonlinear model[3,4] for high oblique ion incidence where a shadowing effect is dominant to describe the surface morphology with respect to the pattern formation of an ion eroded surface.

ACKNOWLEDGMENTS

We acknowledge Professor Ugo Valbusa of Unitá INFM di Genova, Italy, for valuable discussion. We thank Professor Mlian K. Sanyal and Professor Satya R. Bhattacharyya for showing interest in this work. Finally, we would like to thank Subir Roy, Souvik Banerjee, and Chandan Roy for their technical assistance in using the ion implanter and to Avijit Das for his competent help in the AFM work.

*Electronic address: tapas@surf.saha.ernet.in

[1] S. Rusponi, G. Costantini, F. Buatier de Mongeot, C. Boragno, and U. Valbusa, Appl. Phys. Lett. **75**, 3318 (1999).
[2] R. M. Bradley and J. M. E. Harper, J. Vac. Sci. Technol. A **6**, 2390 (1988).
[3] R. Cuerno and A. L. Barabasi, Phys. Rev. Lett. **74**, 4746 (1995); R. Cuerno, H. A. Makse, S. Tomassone, S. T. Harrington, and H. E. Stanley, *ibid.* **75**, 4464 (1995).
[4] M. A. Makeev and A. L. Barabasi, Appl. Phys. Lett. **71**, 2800 (1997); M. A. Makeev, R. Cuerno, and A. L. Barabasi, Nucl. Instrum. Methods Phys. Res. B **197**, 185 (2002).
[5] S. Rusponi, G. Costantini, C. Boragno, and U. Valbusa, Phys. Rev. Lett. **81**, 2735 (1998); **78**, 2795 (1997).
[6] A. L. Barabasi and H. E. Stanley, *Fractal Concepts in Surface Growth* (Cambridge University Press, Cambridge, 1995).
[7] P. Sigmund, Phys. Rev. **184**, 383 (1969); J. Mater. Sci. **8**, 1545 (1973).
[8] Y. Kuramoto and T. Tsuzuki, J. Mater. Sci. **55**, 356 (1977); G. I. Sivashinsky, Acta Astronaut. **6**, 569 (1979).
[9] S. Park, B. Kahng, H. Jeong, and A.-L. Barabasi, Phys. Rev. Lett. **83**, 3486 (1999).
[10] M. Rost and J. Krug, Phys. Rev. Lett. **75**, 3894 (1995).
[11] M. Kardar, G. Parisi, and Y.-C. Zhang, Phys. Rev. Lett. **56**, 889 (1986).
[12] J. Kim, B. Kahng, and A. L. Barabasi, Appl. Phys. Lett. **81**, 3654 (2002).
[13] B. Kahng, H. Jeong, and A.-L. Barabasi, Appl. Phys. Lett. **78**, 805 (2001); S. Facsko, T. Dekorsy, C. Coerdt, C. Trappe, H. Kurz, A. Vogt, and H. L. Hartnagel, Science **285**, 1551 (1991); R. Gago, L. Vazquez, R. Cuerno, M. Varela, C. Ballesteros, and J. M. Albella, Appl. Phys. Lett. **78**, 3316 (2001).
[14] A. K. Hartman, R. Kree, U. Geyer, and M Kölbel, Phys. Rev. B **65**, 193403 (2002).
[15] J. Erlebacher, M. J. Aziz, E. Chason, M. B. Sinclair, and J. A. Floro, Phys. Rev. Lett. **82**, 2330 (1999).
[16] S. Habenicht, W. Bolse, K. P. Lieb, K. Reimann, and U. Geyer, Phys. Rev. B **60**, R2200 (1999).
[17] G. Carter and V. Vishnyakov, Phys. Rev. B **54**, 17 647 (1996).
[18] T. K. Chini, D. Datta, S. R. Bhattacharyya, and M. K. Sanyal, Appl. Surf. Sci. **182**, 313 (2001).

[19] T. K. Chini, M. K. Sanyal, and S. R. Bhattacharyya, Phys. Rev. B **66**, 153404 (2002).
[20] J. E. Van Nostrand, S. J. Chey, M.-A. Hasan, D. G. Cahil, and J. E. Green, Phys. Rev. Lett. **74**, 1127 (1995).
[21] J. Lapujoulade, Surf. Sci. Rep. **20**, 191 (1994).
[22] J. Kim, D. G. Cahill. and R. S. Averback, Phys. Rev. B **67**, 045404 (2003).
[23] H. N. Yang, Y. P. Zhao, A. Chan, T. M. Lu, and G. C. Wang, Phys. Rev. B **56**, 4224 (1997).
[24] Available from www.srim.org
[25] A. C. T Chan and G. C. Wang, Surf. Sci. **414**, 17 (1998).
[26] G. Carter, J. Appl. Phys. **85**, 455 (1999).
[27] J. J. Vajo, R. E. Doty, and E. H. Cirlin, J. Vac. Sci. Technol. A **14**, 2709 (1996).
[28] K. Wittmaack, J. Vac. Sci. Technol. A **8**, 2246 (1990).
[29] M. Siegert and M. Plischke, Phys. Rev. E **50**, 917 (1994).
[30] D. E. Wolf and J. Villain, Europhys. Lett. **13**, 389 (1990).
[31] S. M. Rosnagel, R. S. Robinson, and H. R. Kaufman, Surf. Sci. **123**, 89 (1982).
[32] D. Flamm, F. Frost, and D. Hirsch, Appl. Surf. Sci. **179**, 95 (2001).
[33] S. Rusponi, G. Costantini, C. Boragno, and U. Valbusa, Phys. Rev. Lett. **81**, 4184 (1998).
[34] T. K. Chini, F. Okuyama, M. Tanemura, and K. Nordlund, Phys. Rev. B **67**, 205403 (2003).